Scanning Microscopy

Volume 5 | Number 2 Article 1

5-24-1991

Backscattered Electron Imaging for High Resolution Surface Scanning Electron Microscopy with a New Type YAG-Detector

Paul Walther
University of Wisconsin-Madison

Rudolf Autrata
Czechoslovak Academy of Science

Ya Chen
University of Wisconsin-Madison

James B. Pawley
University of Wisconsin-Madison

Scanning Microscopy, Vol. 5, No. 2, 1991 (Pages 301-310)
Scanning Microscopy International, Chicago (AMF O'Hare), IL 60666 USA

0891-7035/91$3.00+.00

BACKSCATTERED ELECTRON IMAGING FOR HIGH RESOLUTION SURFACE SCANNING ELECTRON MICROSCOPY WITH A NEW TYPE YAG-DETECTOR

Paul Walther[1]*, Rudolf Autrata[2], Ya Chen[1], James B. Pawley[1]

1: Integrated Microscopy Resource for Biomedical Research
University of Wisconsin-Madison
1675 Observatory Drive, Madison, WI, 53706, USA
2: Institute of Scientific Instruments
of the Czechoslovak Academy of Sciences
Kralovopolska 147, 612 64 Brno, Czechoslovkia

(Received for publication January 18, 1991, and in revised form May 24, 1991)

Abstract

Double Layer Coating for backscattered electron imaging is a coating and imaging method especially suitable for high resolution scanning electron microscopy (SEM) of large biological samples. Since the backscattered electron (BSE) signal from thin metal coating layers is quite low, field emission SEM's and very sensitive BSE-detectors are required for this method. In this study an improved BSE-detector of the YAG type was used with an in-lens type field emission SEM. Two samples were investigated in order to demonstrate and to improve the potential of this new approach: (1) cryo-prepared cultured kidney cells were shadowed by electron beam evaporation with platinum-carbon (unidirectionally at a fixed angle of 45°) and then coated with an additional 10 nm carbon layer; and (2) cryo-prepared trichocyst matrixes (paracrystalline structures contained in secretory granules, the trichocysts, found in *Paramecium*) were coated by ion beam sputtering with about 1 nm of platinum. This sample was rotated and tumbled during coating in order to obtain as uniform a metal layer as possible and then an additional 10 nm carbon layer was evaporated over the metal. When these samples were viewed at a primary beam accelerating voltage (V_o) of 10 kV or higher, contrast was good on the unidirectionally coated cell culture samples. However, trichocyst matrixes with the thinner and more uniform coating showed very poor contrast because most of the BSE detected represented beam-specimen interactions from the bulk of the sample and not in the thin platinum layer. The situation was improved by using low V_o (4 kV). Under these conditions the penetration depth of the electrons is reduced and a greater proportion of the BSE electrons are scattered by the platinum layer. The results were compared with freeze-fracture and deep-etch transmission electron microscope studies of the trichocyst matrixes from the literature: Almost similar resolution is achieved on the biological structures but a better impression of the three dimensional arrangement of the whole trichocyst matrix is obtained with the SEM. The globular particles form disc-like structures that are connected with each other by thin fibers.

Key Words: Scanning Electron Microscopy, Backscattered Electrons, Low Voltage, Yttrium Aluminum Garnet detector, ion beam sputtering, Double Layer Coating, freeze-substitution, trichocyst matrix.

***Address for correspondence:**
Paul Walther / IMR / University of Wisconsin-Madison
1675 Observatory Drive / Madison, WI, 53706
Phone# (608) 263 8481 Fax# (608) 262 4570

Introduction

Backscattered electron (BSE) imaging has three major applications in the SEM of biological specimens: 1. Heavy metal precipitates in cells produced by cytochemical reactions are visualized with the material-dependent BSE-signal (Becker and Sogard, 1979; Small et al., 1980; Vandenburgh et al. 1987; and others). 2. Colloidal gold particles used as markers for affinity labeling can be detected with the BSE-image on biological surfaces (Trejdosiewicz et al., 1981; Walther et al, 1983 and 1984, de Harven et al., 1984 and others; reviewed by Mueller et al., 1989). Labelling efficiency may be increased by the use of smaller gold markers (Slot and Geuze, 1984). However the BSE-signal decreases with the decreasing mass of the particles. So, in order to detect particles in the size range of 1 to 5 nm very efficient BSE-detectors are required. (Mueller and Hermann, 1990a and 1990b; Walther and Mueller, 1985). 3. The BSE-signal can also be used to show surface structures highlighted by directional metal shadowing with high resolution (Walther and Hentschel, 1989). This new approach has several advantages compared to the secondary electron image usually used especially on large biological samples. Biological specimens are electrical insulators. In order to avoid charging artifacts, electrical conductivity is usually produced by coating with a metal layer. To avoid hiding of small structural details, the thickness of such a layer should be less than the desired resolution. So, in order to detect macromolecular features, coating layers in the nm range are needed. Unfortunately, the electrical conductivity of layers this thin is poor, especially on large, rough samples where electrical conductivity must be maintained over relatively large distances (millimeters).

Since modern, in-lens field emission SEM's provide probe diameters below 1 nm (Nagatani et al., 1987), many efforts have been undertaken to overcome the limitations mentioned above: 1. Developing more uniform coatings to provide better electrical conductivity (Echlin, 1981; Echlin et al., 1985; Peters, 1986; Hermann et al., 1988; Mueller and Hermann 1990a and 1990b; Wepf and Gross, 1990 and others); 2. Enhancing the conductivity of the biological sample by extensive staining with heavy metals (Tanaka and Mitsushima, 1984; Tanaka et al., 1989), and 3. Use of low V_o (typically 1.5 kV) to reduce charging on samples coated with very thin layers (below 1 nm) that therefore have poor electrical conductivity (Thornley, 1960; Pawley and Erlandsen 1989; Pawley, 1990; Osumi et al., 1988 and 1990). This method has become an interesting approach for high-resolution SEM since new in-lens field emission SEM's providing very small probe diameters even at low V_o have become available (Pawley, 1990; Sato et al., 1990).

Another strategy to overcome these problems is Double Layer Coating and BSE-imaging (Walther and Hentschel, 1989). The basic idea is to provide two separate coatings: one to provide contrast formation and the other for electrical conductivity. To do this the specimen is first coated with a thin (e.g. 2 nm or less) directional layer of a heavy metal (e.g. platinum-carbon) and then this is backed with an additional carbon layer of about 10 nm. When such a sample is imaged with BSE, the contrast is mainly produced at the thin layer of heavy metal whereas electrical conductivity and mechanical stability are provided by the overlying carbon coat. The method has enabled the visualization of macromolecular particles on large pieces of kidney tissue (Herter et al, 1991; Walther et al., 1990). Even though Double Layer Coating was mainly developed for large samples, Mueller and Hermann (1990b) have shown that, on an isolated protein layer, it produces a resolution equally good to that provided by the best coating procedures for secondary electron 1 (SE1) imaging. (SE1 are the secondary electrons produced at the site where the primary beam enters the specimen. They carry the high resolution information about the sample surface. Reviewed by Joy, 1991.)

Because little BSE-signal is produced by scattering from a 2 nm metal layer (reviewed by Niedrig, 1978; Joy, 1984; Luo and Joy, 1988) this application requires very sensitive BSE-detectors. However, when crossing a thin layer, a low V_0 electron is more likely to be scattered than a high V_0 electron. This means that, for a thin metal layer, the BSE yield increases as V_0 is lowered, and seeing the particles in such a layer is easier at low V_0 as long as the BSE-detector can still operate efficiently.

In this study an improved YAG-type BSE-detector (Autrata, 1991) was used in a high resolution, in-lens type field emission SEM (Nagatani et al., 1987). YAG-type scintillator BSE-detectors (reviewed by Autrata, 1989) have a number of advantages: The scintillators have high efficiency, an unlimited lifetime, can be produced in almost any desired shape and their cathodoluminescence has a very short decay time enabling the use of rapid scan speeds. Recent improvements involve the use of conductive, diffusive and reflective coatings applied to the surface of these scintillators to prevent surface charging and to transmit a greater fraction of the light produced, to the photomultiplier tube. Recently, using this type of detector in a field emission in-lens SEM Mueller and Hermann (1990a and 1990b) were able to detect 1 nm gold particles with the BSE signal.

The goals of this work were: 1. Comparison of the results obtained with the new detector in an in-lens type microscope with results described previously with a below-the-lens SEM (Walther and Hentschel, 1989; Herter et al., 1991); 2. Extension of the Double Layer Coating approach to specimens that have been uniformly coated rather than shadowed, and 3. Determination of the optimal V_0 for this technique.

The following specimens were used: 1. A renal epithelial cell line in culture (LLC-PK_1), and 2. Isolated, discharged trichocyst matrixes.

The trichocyst matrix is an ordered protein structure, initially contained in a membrane-bound organelle, the trichocyst found in large numbers just beneath the cell membrane of *Paramecium* . When triggered by electrical or mechanical stimulation it is exocytosed and expands to about 8 x its original length in a few milliseconds. The structure of the condensed and expanded (discharged) forms has been well studied in the TEM by negative-stain, by thin-sectioning and by freeze-fracture deep-etch techniques (Bannister, 1972; Hausmann, 1972; Peterson et al., 1987; Sperling et al., 1987 and others).

The reasons for choosing these specimens were as follows: 1. The cultured kidney cells had already been investigated in previous studies (Walther and Hentschel, 1989) using the same preparation protocol (fast-freezing, freeze-substitution and critical point drying; Barlow and Sleigh, 1979) with a below-the-lens field emission SEM. It could be shown that large surface areas (mm^2's) are preserved allowing imaging at low magnification for better orientation. It would be much more difficult and tricky to visualize these structures with any other technique (e.g. TEM surface-replicas; Hohenberg et al., 1986). 2. The trichocyst matrix has a three-dimensional, periodic structure. The two-dimensional appearance is well described in the TEM studies mentioned above. These studies provided reference images with which to compare our results from the SEM. In addition, the high resolution SEM could give more information about the three-dimensional arrangement of the entire trichocyst matrix structure and its interaction with the substrate, something which is difficult to obtain with the TEM.

Material and Methods

Kidney epithelial cells in culture: LLC-PK_1 cells grown on thermanox coverslips were prepared as described by Walther and Hentschel (1989). The cells in contact with the culture medium were fast frozen by plunging into liquid propane cooled by liquid nitrogen. Freeze substitution was carried out as described by Mueller et al. (1980) and by Walther and Hentschel (1989): The freeze-substitution medium consisted of methanol containing 0.5% osmium tetroxide, 3% glutharaldehyde and 3% water. Samples were freeze-substituted in a Balzers FSU 010 for 7 h at 183 K, 5h at 213 K and 5h at 243 K. After washing with cold methanol (243 K), samples were warmed up to room temperature, washed with ethanol and critical point dried (Anderson, 1951; Barlow and Sleigh, 1979) as described by Ris (1985) using carbon dioxide.

The cell culture specimens were coated in a Balzers BAF-300 by electron beam evaporation (Moor, 1973) with 2 nm of platinum-carbon at an angle of 45^{o} and backed with a 10 nm carbon layer evaporated at 90^{o} to the surface. The film thickness was measured with a quartz crystal thickness monitor.

Trichocyst matrixes: Carbon stubs (diameter: 3 mm) were incubated with a small droplet of the discharged trichocyst matrix suspension for about 2 min and frozen by plunging into liquid ethane, cooled to a temperature of about 110 K by liquid nitrogen, and then stored in liquid nitrogen. Freeze substitution and critical point drying were carried out as described above. The trichocyst matrix samples were coated with platinum by ion beam evaporation (Franks et a., 1980) in an Ion Tech apparatus. The thickness estimate of 1 nm is based on the final BSE images as explained in the discussion. The coating conditions were: Argon pressure in the specimen chamber: 2×10^{-5} mbar; time: 6 min; Ar^{+} beam current: 4 mA at 10 kV. The specimen was rotated and tumbled during coating. After platinum coating, specimens were coated with an additional layer of carbon with a thickness of 5 to 10 nm by indirect evaporation.

Scanning electron microscopy and BSE-Detector: A Hitachi S-900, in-lens, field emission SEM (Nagatani et al., 1987) with modifications to enhance the performance of the microscope at low V_0 (Pawley, 1990; Pawley and Erlandsen, 1989) was used. To minimize hydrocarbon residues in the vacuum, all rough pumping was performed by oil-free molecular drag pumps (Danielson, 1987).

Fig. 1. Cultured kidney epithelial cells (LLC-PK1) Double Layer Coated with 2 nm of platinum-carbon (unidirectionally) and then 10 nm of carbon (for details see text). The backscattered electron image is obtained at a V_0 of 10 kV. The 2 nm platinum layer provides a sufficiently high BSE-signal to image cell surface structures such as the cell membrane with microvilli.

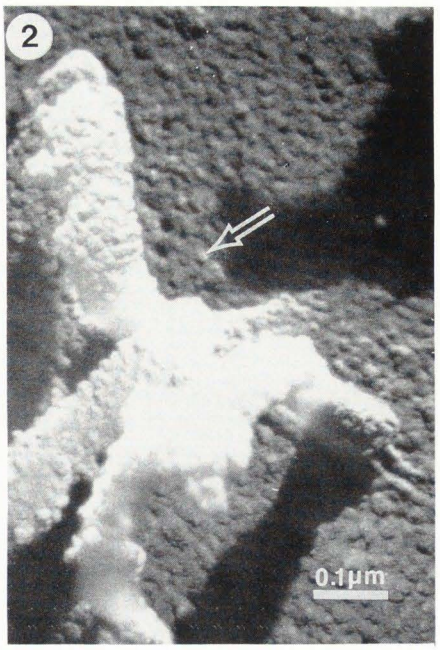

Fig. 2. The same sample at higher magnification (x100,000). The microvilli and the membrane in between are covered with particles (large arrow, diameter 10 to 30 nm) most probably representing proteins or carbohydrate chains of glycoproteins.

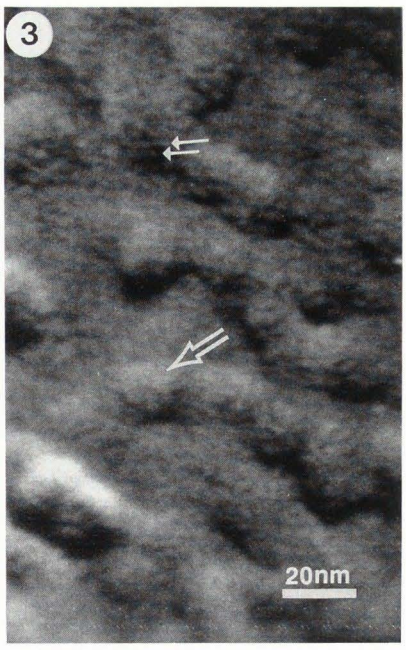

Fig. 3. The same sample at very high magnification (x 500,000). The 10 to 30 nm particles (large arrow) show a finer substructure with a size in the range of 2 nm (small arrows) which probably represent the individual platinum clusters. Whether this substructure represents a decoration effect that corresponds with an underlying biological structure or the platinum clusters are randomly distributed is not known.

The YAG-detector is similar to that described by Autrata et al. (1986) with some improvements: Electrical conductivity of the YAG-crystal is not achieved by coating with aluminum but by chemical treatment using indium and tin oxide. The aluminum film on the light guide surface is removed and replaced by an aluminum foil. Some places of the scintillator are coated by deposition with an antireflecting layer or are additionally covered with a diffusion layer. These modifications lead to a higher sensitivity and especially enable the detection of a BSE-signal with a V_0 as low as 1.5 kV (Autrata, 1991).

All figures shown are BSE-images, except Fig. 11 which is a secondary electron image. V_0 was 4 kV unless stated otherwise. The beam current (at V_0=4 kV) was approximately 2 to 3 x 10^{-10}A. Scanning speed during exposure was 80 s, except for Fig. 7, 8 and 9 where it was 40 s.

Results

The cultured kidney epithelial cells (Fig. 1) show high contrast in the BSE-mode at V_0=10 kV, even at low magnifications, and the microvilli covering the cell surface are visible. At a magnification of 100,000 x (Fig.2) the cell surface appears covered with particles (large arrow, sizes between 10 and 30 nm). At very high magnifications (500,000 x; Fig. 3) an even smaller pattern in the 2 nm range becomes visible (small arrows).

As expected, the contrast on the more uniformly coated trichocyst matrixes is much lower than in the unidirectionally coated samples, especially at low magnifications. However, as seen in Figs. 4 to 6, the situation depends heavily on V_0: With 30 kV or 20 kV, surface structures are hardly visible (Figs. 4 and 5), but when V_0=4 kV (Fig. 6) the platinum coated surface structures appear with high contrast. At very high magnifications (500,000 x; Figs. 7 to 9) the grain of the platinum film becomes visible. Again, at 30 kV (Fig. 7) the BSE-signal of the platinum layer is relatively low. At 20 kV (Fig. 8) and at 4 kV (Fig. 9) the BSE-signal from the platinum is increased. At V_0=4 kV (Fig. 9) the grains can still easily be resolved but they appear to be slightly enlarged because of the larger diameter of the primary beam. When a V_0 below 4 kV was used the high magnification image became blurred and it was difficult to resolve the platinum grains (not shown). Therefore, it was concluded that 4 kV was the most suitable V_0 to image the uniformly coated samples with the equipment used for this study.

Figs. 10 and 11 demonstrate the advantage of using the BSE signal when imaging a Double Layer Coated sample: The thin platinum layer is only visible with BSE (Fig. 10) because they can penetrate the outer carbon coating. Secondary electrons (Fig. 11) come from the surface of the carbon coat covering the specimen and this coating obscures small structural details. Therefore, the width of the fibers appears to be much smaller in the BSE-mode (white arrows in Fig. 10) than in the SE-mode (black arrows in Fig. 11).

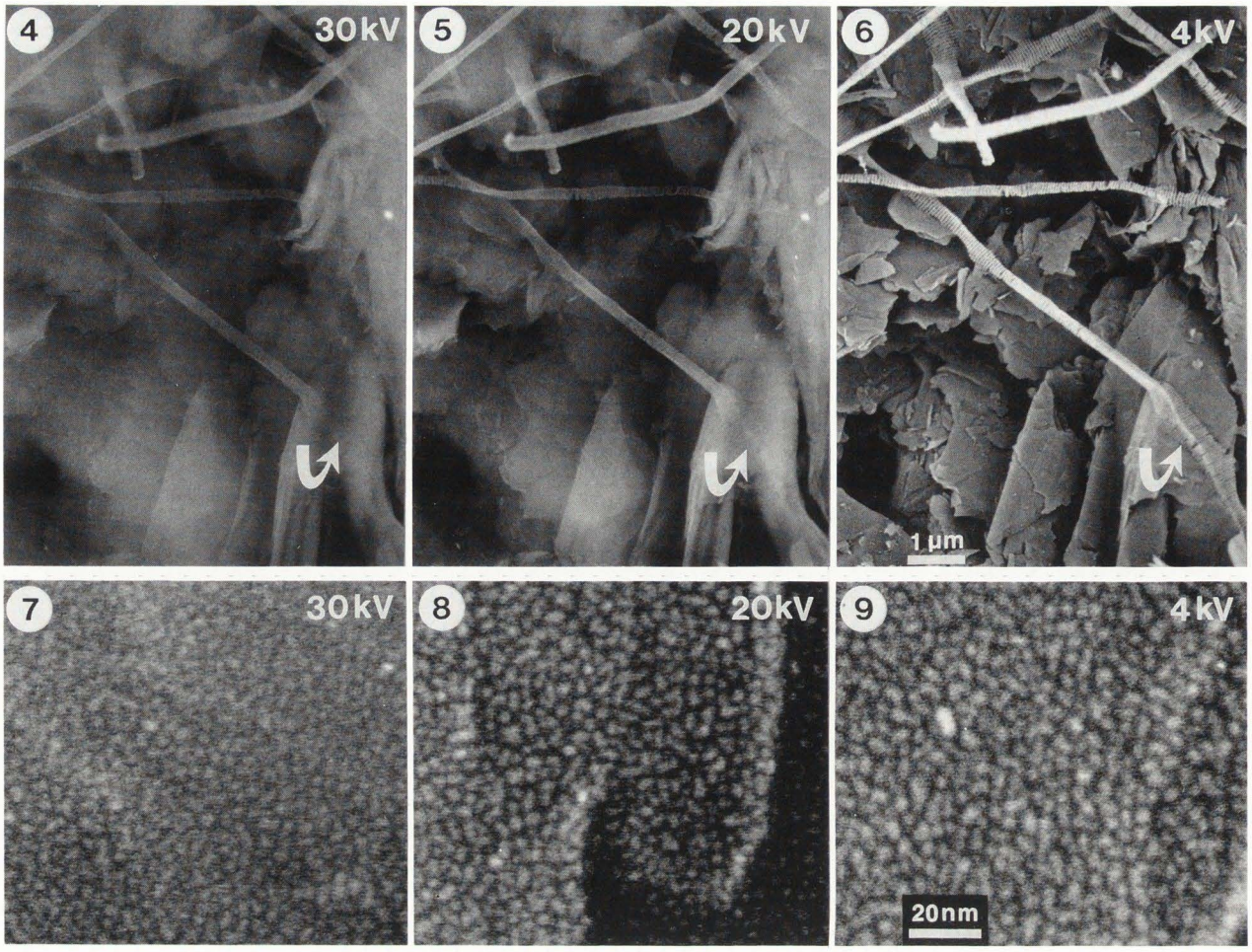

Figs. 4, 5, and 6. Low magnification BSE-images of the same group of trichocyst matrixes deposited on a carbon substrate and Double Layer Coated with about 1 nm of platinum (uniformly; by ion beam sputtering) and with about 10 nm of carbon. The differences evident demonstrate the influence of V_o (Fig. 4 = 30 kV; Fig. 5 = 20 kV; Fig. 6 = 4 kV). The fraction of the signal derived from the platinum layer is increased at low V_o because proportionally more electrons are scattered by this thin layer and the trichocyst matrixes on the carbon surface (arrows) become more visible.
Figs. 7, 8, and 9. The same sample (as Fig. 4, 5 and 6) at very high magnification (x 500,000) at different values of V_o (Fig. 7 = 30 kV; Fig. 8 = 20 kV; Fig. 9 = 4 kV). At low V_o (Fig. 9), as expected, resolution is slightly decreased. The increased probe diameter and greater scattering by the overlaying carbon coat cause the platinum clusters seem larger. Nevertheless, the individual clusters (with a diameter of approximately 2 nm and an estimated average thickness of 1 nm) are still clearly resolved.

A stereo pair showing three trichocyst matrixes is seen in Fig. 12. As described in the literature, the trichocyst matrix structure consists of macromolecules arranged in parallel striations. These striations are connected by very thin fibers. In the trichocyst matrix viewed side-on , the distance between the striations is exactly 55 nm as described in freeze-etch replica studies (Peterson et al. 1987, Sperling et al. 1987). In the horizontally arranged trichocyst matrix, however, the mean distance is around 45 nm. The uppermost trichocyst matrix is broken and the three-dimensional structure of the "striations" can be recognized: The subunits are arranged in discs. This arrangement becomes even more obvious in the disordered sample shown in Fig. 13.

Fig. 14 represents a high magnification (x 200,000) stereo pair. The discs are formed by many globular-shaped particles each with a diameter of about 20 nm. Sometimes parts of the surface are fractured away and the internal structure becomes visible (asterisk).

The trichocyst matrixes tend to attach and spread on the carbon substrate (Fig. 15) and this process can produce structural changes. It seems that the outer layer of the trichocyst matrix opens so that the inside of this layer can attach to the substrate.

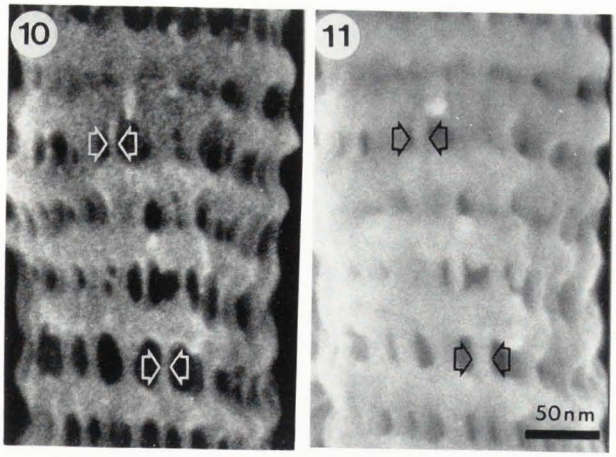

Figs. 10 and 11. A Double Layer Coated trichocyst matrix imaged with the BSE signal (Fig. 10) and the secondary electron signal (Fig. 11). The BSE signal (Fig. 10) images only the thin platinum coat and the apparent diameter of the fibers is very small (white arrows). In the secondary electron mode (Fig. 11) the surface of the overlaying carbon coat is imaged, fine structural details are obscured and the apparent diameter of the fine fibers is enlarged (black arrows).

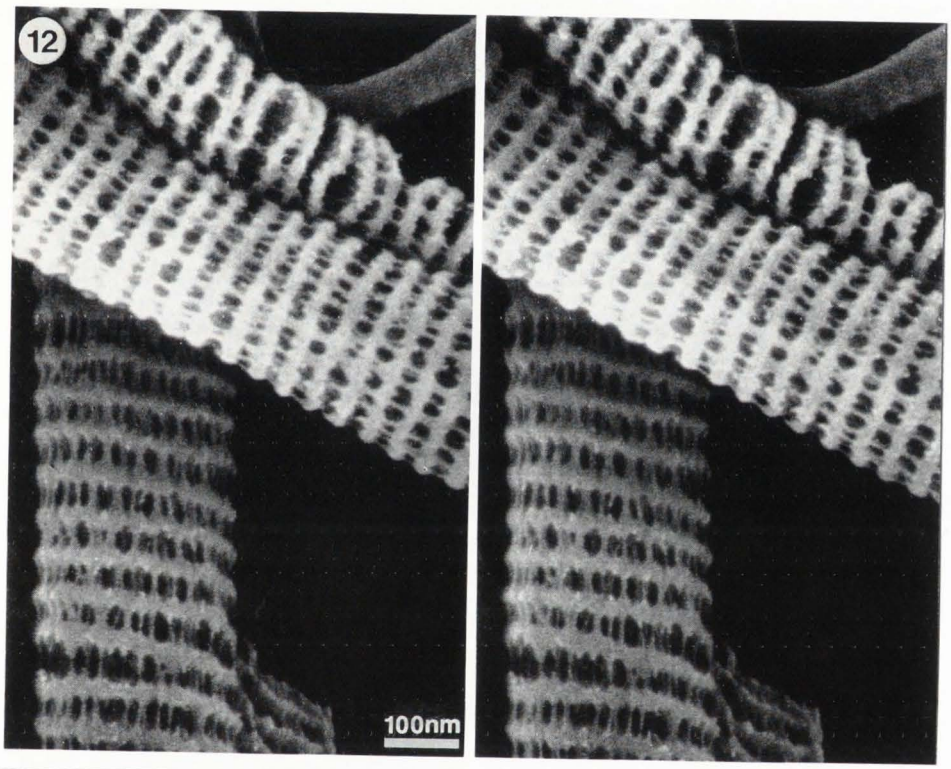

Fig. 12. Stereo pair showing the trichocyst matrix structure. The paracrystaline lattice made up of individual macromolecules is arranged in discs that are connected with each other by very thin fibers. The trichocyst matrix at the top is broken and the arrangement of the macromolecules in discs becomes more obvious.

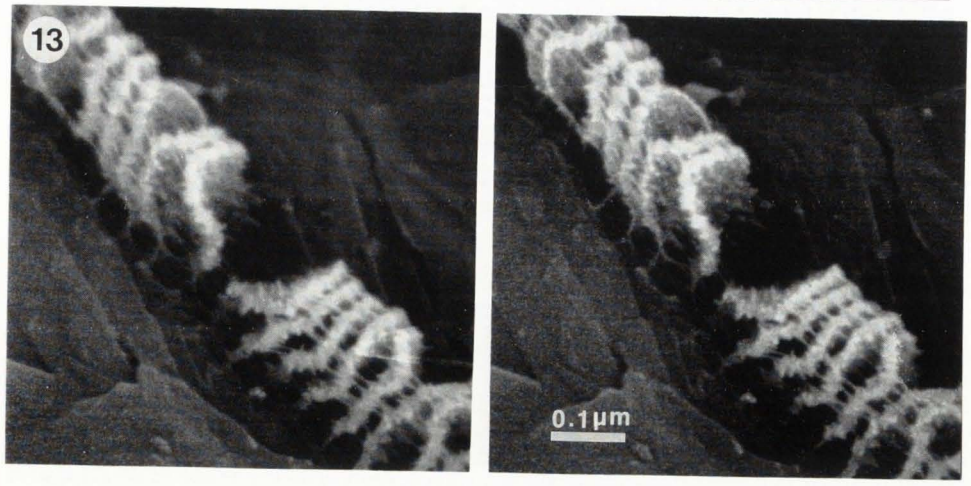

Fig. 13. This trichocyst matrix was probably ruptured during preparation. The form of the fracture implies that the trichocyst matrix is composed of disc-like structures, held together by thin fibers which have partially been broken in this sample.

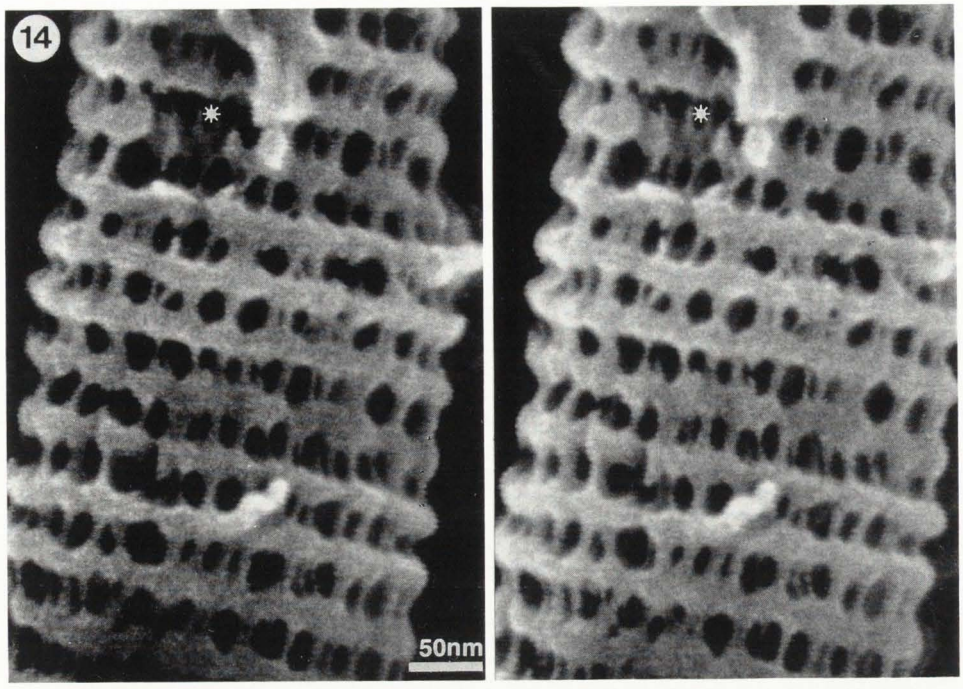

Fig. 14. High magnification (x 200,000) stereo pair of a Double Layer Coated trichocyst matrix imaged with BSE. The discs are composed of globular-shaped particles with a diameter of about 20 nm most likely representing macromolecules. The asterisk denotes a region where the outermost layer is fractured away and the inside is visible.

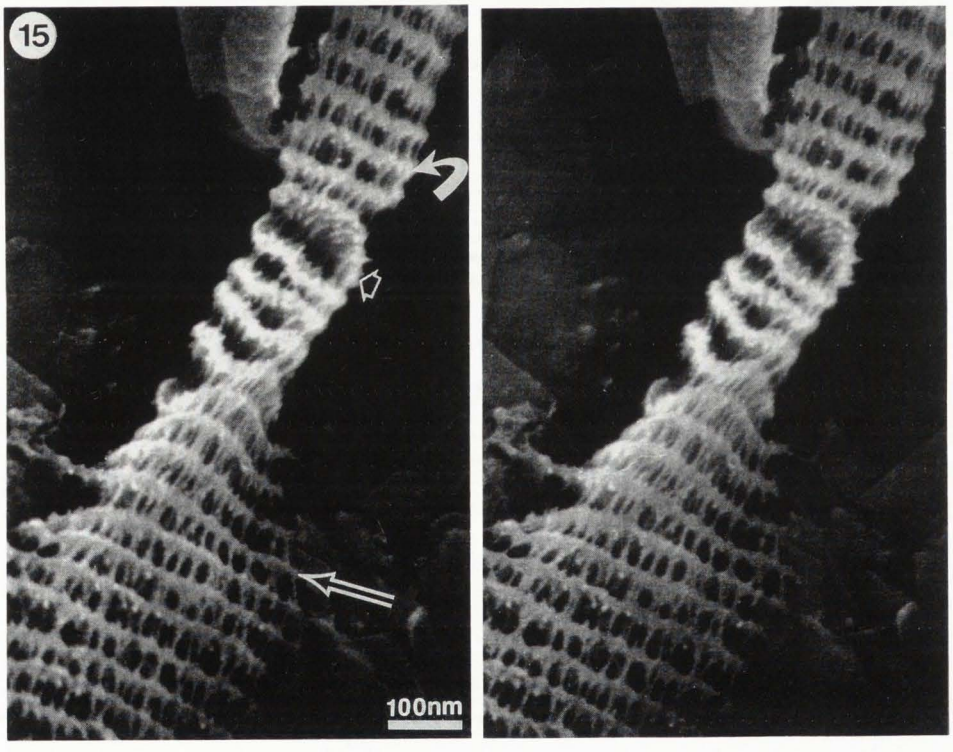

Fig. 15. The trichocyst matrixes tend to attach and spread on the carbon substrate. This stereo pair shows three different structural states. The curved arrow denotes the intact trichocyst matrix structure. The short arrow points to a region with a lot of ruptured thin fibers, the arrangement of the macromolecules in discs becomes visible. The long arrow marks a part that is attached and spread on the carbon substrate before cryofixation. The outer layer of the trichocyst matrix appears to have opened so that the inside of this layer can adhere to the substrate.

Discussion

The purpose of this work is to investigate the potential of Double Layer Coating and BSE-imaging combined with a high resolution, in-lens field emission SEM equipped with a sensitive BSE-detector. One advantage of the in-lens SEM is high resolving power even at low V_0. As demonstrated in Figs. 3 and 6, the new Autrata YAG-detector is much more sensitive at low V_0 than earlier detectors. The advantages of low V_0 for surface imaging with secondary electrons have been extensively studied and reviewed (Pawley, 1990; Pawley and Erlandsen, 1989; Osumi et al., 1988 and 1990). Many of these advantages also apply when the BSE-signal is collected: The primary beam penetrates less deeply into the specimen. Therefore, more scattering events take place close to the surface particularly in the heavy metal layer that contains the high resolution information. This provides higher image contrast and has the result that an image can be obtained with

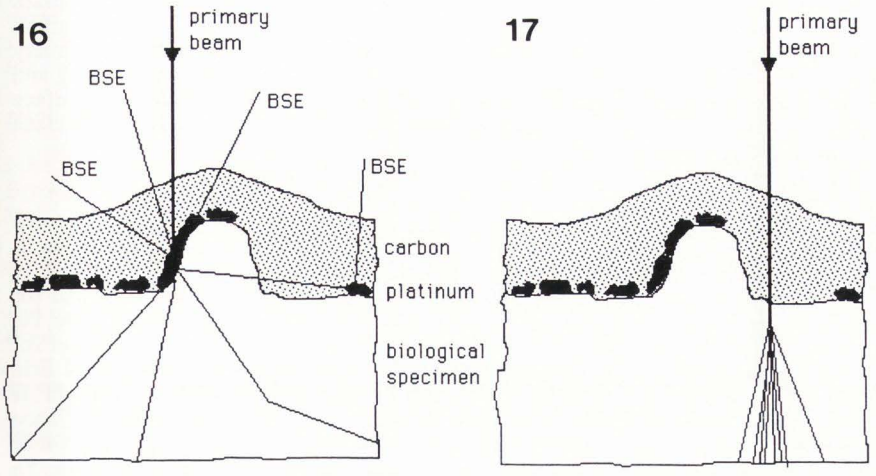

Fig. 16 and 17. Diagram of BSE-contrast formation on a unidirectionally platinum coated specimen (such as Figs. 1 to 3). In Fig.16 the primary beam hits the platinum, a lot of BSE are produced and a high BSE-signal is detected. In Fig. 17 the primary beam is in a platinum-free region (in the shadow of the platinum evaporation source) and therefore no BSE are produced at the specimen surface. A high BSE-contrast is produced by a unidirectionally coated sample.

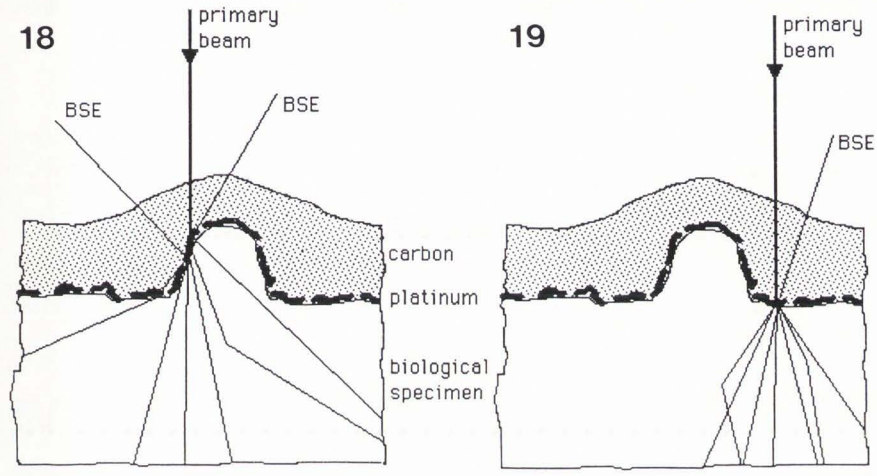

Fig. 18 and 19. Diagram of BSE contrast formation on a more uniformly platinum coated sample (such as Figs. 4 to 15). In Fig. 18 the primary beam hits the platinum layer at a low angle, the path of the electrons in the platinum layer is relatively long and the probability of electrons to be scattered is high. In Fig. 19 the primary beam hits the platinum layer perpendicularly. The path of the electrons in the platinum layer is shorter and less BSE are produced than in Fig.18. However, the difference in the BSE coefficient between the two areas is still less than it is on the unidirectionally shadowed specimen and the image contrast is less.

less radiation damage to the specimen (Pawley et al., 1991). In addition, more electrons leave the surface, and the net charge deposition is reduced resulting in less charging problems (Pawley, 1972).

The highest image contrast is obtained on samples which had been unidirectional coated ("shadowed"; Fig. 1 to 3) because structures in the "shadow" of the platinum beam remain uncoated and the mass-dependent BSE-signal varies strongly between coated and uncoated parts of the specimen (Figs. 16 and 17). When a more uniformly coated sample is imaged (Fig. 4 to 15), contrast depends on the angle between the platinum coat and the primary beam, the so called "topologically dependent mass thickness" (Joy; 1987; Figs. 18 and 19). In this case contrast is lower than on a "shadowed" sample, but because of the high sensitivity of the BSE-detector, at low voltages, it is still sufficient. We found V_0=4 kV the most suitable primary accelerating voltage to image the uniformly coated samples with our equipment (in-lens field emission SEM). At this V_0 the diameter of the primary beam is still small enough to resolve the platinum grains. We do not expect to preserve biological structures smaller than the grain size. Therefore the grain size is the limiting factor of our approach and not the resolution of the microscope at 4 kV. However, when a V_0 below 4 kV was used it became difficult to resolve the platinum grains. We assume that at V_0 below 4 kV several effects limit the resolution of a double layer coated specimen: 1. The diameter of the primary beam increases, 2. more electrons are scattered at the overlaying 5 to 10 nm carbon layer and 3. the sensitivity of the BSE-detector drops below 3 kV.

The thin, ion-beam sputtered platinum film is obviously far from uniform. It forms a grainy pattern on the surface of the sample that can be resolved with the BSE signal at very high magnifications (Figs. 4 to 6). These coating patterns have been extensively investigated on transparent films in the TEM. Wildhaber et al. (1985) measured the thickness of ion-beam sputtered films with a quartz crystal monitor. They observed the individual grains starting to grow together at an average film thickness of about 1 nm. Since the grains in our films are not grown together and the distribution and the size of the grains correspond very well with their image of a 1 nm ion-beam-sputtered platinum film (their Fig. 2C) we estimate that our average film thickness is about 1 nm. This also corresponds well with data published by Lindroth and Sundgren (1989, their Fig 2A). However, both authors obtained finer grained films using other metals than platinum, such as tungsten or germanium. Whether tungsten films are useful for SEM BSE-imaging and whether they preserve the shape of biological structures to a higher resolution has to be shown in future.

Wildhaber et al. (1985) compared ion-beam sputtering versus electron gun evaporation. They came to the conclusion

that metal from an electron gun tends to decorate the substrate more. Though this leads to more diffraction points on a periodic sample, indicating a higher resolution. However, it is not clear that decoration effects provide information useful for the interpretation of biological structures because not much is known about the nature of the decorated sites.

In this study, we have used only bulk samples that do not transmit the electron beam. Initially, we were concerned that the BSE-signal derived from the bulk of the specimen might obscure the signal from the platinum layer. This is obviously not the case. By comparing the results presented with those obtained with platinum films on transparent collodium films (data not shown) no major difference in resolution or image contrast can be observed.

We can also confirm that, as pointed out by Ris (1985), proper critical-point-drying is a crucial step in the preparation protocol. The smallest amounts of water in the critical point drying chamber lead to tremendous artifacts (not shown) and macromolecular structures can no longer be observed.

The study of trichocyst matrix structure most comparable to our own was done by Peterson et al. (1987) using the slam-freeze, deep-etch replica technique. This TEM technique also is based on fast freezing as the initial fixation step and uses metal coating. We believe that in many ways our results are quite similar to these freeze-etch data even though our protocol involves the use of additional dehydration and drying procedures (freeze-substitution and critical-point-drying): In both, the substructure of the trichocyst matrixes consists of a paracrystalline pattern arranged in parallel striations which are connected by thin fibers. According to the literature (Hausmann et al., 1972; Bannister, 1972; Peterson et al., 1987; Sperling et al., 1987) the distance between two lines is 55 nm. In our samples, however, the distance varies from about 45 to 55 nm. One possible reason for this discrepancy could be shrinkage during dehydration by freeze-substitution or drying by critical-point-drying. It is generally accepted that freeze-substitution causes less structural changes than dehydration at room temperature, but one should keep in mind that the removal of water always causes some shrinkage (Boyde and Franc, 1981; MacKenzie, 1972).

We believe that the SEM approach has the advantage of a better representation of the three-dimensional structure on the intermediate magnification scale (i.e. whole trichocyst matrixes). The arrangement of the trichocyst matrix molecules in discs originally suggested by Hausmann, 1972 becomes obvious in the SEM (Figs. 13 and 14) but is difficult to recognize with any other method. Also the way the trichocyst matrixes spread out when attaching an active surface (Fig. 15) becomes very clear in an SEM stereo image. The image of a replica or of a negative stained sample in the TEM does not indicate whether a trichocyst matrix is in solution or has attached and spread. Fig. 15 also demonstrates that a structure can undergo severe changes by attaching to a surface. This should be kept in mind when using active surfaces as substrate such as glow discharged carbon foil or mica chips.

Conclusions

Trichocyst matrixes are prepared by cryo-fixation, freeze-substitution, critical-point-drying, coating with 1 nm of platinum and about 10 nm of carbon. Reasonably good contrast was obtained with the backscattered electron signal at a low V_o of 4 kV.

Advantages of this approach are: 1. Charging artifacts are avoided even on large samples because the BSE-signal is less affected by specimen charging, the additional carbon coat enhances electrical conductivity, and charging is reduced at low V_o anyway; 2. The platinum layer need not be electrically conductive and can therefore be kept very thin (average thickness:1 nm); 3. The carbon coat mechanicaly stabilizes both the sample and the platinum coat, and 4. Hydrocarbon contamination polymerized onto the surface by the primary beam is much less of a problem than with other coating and imaging modes because BSE's are less affected by surface contamination and the carbon coat provides a relatively clean surface.

Acknowledgment

We thank Shian-Jiun Shih, David L. Nelson and Joan B. Peterson from the Biochemistry Department of the University of Wisconsin for providing the trichocyst samples and for helpful discussions. We thank all the staff members of the Integrated Microscopy Resource for technical help and for generous support. The expert photographic work of Eric Landmark is gratefully acknowledged. Paul Walther is partially supported by a grant of the Swiss National Science Foundation and by a Guyer Postdoctoral Fellowship grant of the Zoology Department of the University of Wisconsin. Ya Chen is supported by the Shanghai Normal University, Peoples Republic of China. This work was also supported by NIH Grant DRR-570 to the Integrated Microscopy Resource, Madison, Wisconsin.

References

Anderson TF. (1951). Techniques for the preservation of three-dimensional structures in preparing specimens for the electron microscope. Trans NY Acad Sci. 13: 130-133.

Autrata R, Walther P, Kriz S, Mueller M. (1986). A BSE-scintillation detector in the (S)TEM. Scanning, 8, 3-8.

Autrata R. (1989). Backscattered electron imaging using single crystal detectors. Scanning Microsc. 3, 739-763.

Autrata R, Hermann R, Mueller M. (1991). An efficient BSE single crystal detector for SEM. Scanning in press.

Bannister LH. (1972). The structure of trychocysts in *Paramecium caudatum*. J Cell Sci. 11, 899-929.

Barlow D I, Sleigh MA. (1979). Freeze substitution for preservation of ciliated surfaces for scanning electron microscopy. J Microsc. 115, 81-95.

Becker RP, Sogard M. (1979). Visualization of subsurface structures in cells and tissues by backscattered electron imaging. Scanning Electron Microsc. 1979; II: 835-870.

Boyde A, Franc F. (1981). Freeze drying shrinkage of glutaraldehyde fixed liver. J Microsc. 122, 75-86.

Danielson P. (1987). Rough pumping without oil contamination. Res Devel. 29, 97-104.

de Harven E, Leung R, Christensen H. (1984). A novel approach for SEM of colloidal gold labelled cell surfaces. J Cell Biol. 99, 53-57.

Echlin P. (1981). Recent advances in specimen coating techniques. Scanning Electron Microsc. 1981; I: 79-90.

Echlin P,Gee W, Chapman B. (1985). Very low voltage sputter coating. J Microsc. 137, 155-169.

Franks J, Clay CS, Pease GW. (1980). Ion beam thin film deposition. Scanning Electron Microsc. 1980, I: 155-162.

Hausmann K. (1972). Cytological studies on trichocysts I: The fine structure of discharged spindle trichocysts in *Paramecium caudatum*. Cytobiologie. 5, 208-227.

Hermann R, Pawley J, Nagatani T, Mueller M. (1988). Double-axis rotary shadowing for high-resolution scanning electron microscopy. Scanning Microsc. 2, 1215-1230.

Herter P, Tresp G, Hentschel H, Zierold K, Walther P. (1991). High resolution scanning electron microscopy of frozen-hydrated and freeze-substituted kidney tissue. J Microsc. 161, 375-385.

Hohenberg H, Bohn W, Rutter G, Mannweiler K.

(1986). Plasma membrane antigens detected by replica techniques. In: Mueller M, Becker RP, Boyde A, Wolosewick JJ (eds) Science of Biological Specimen Preparation, SEM Inc., AMF O'Hare, Chicago, Il 60666-0507, USA. 235-244.

Joy DC. (1984). Beam interactions, contrast and resolution in the SEM. J Microsc. 136, 241-258.

Joy DC. (1987). Low voltage scanning electron microscopy. In: Electron microscopy and analysis, 1987. Brown LM (ed). Inst Phys Conf Ser No. 90: Chapter 7. Institute of Physics, Bristol and Philadelphia: 175-180.

Joy DC. (1991). Contrast in high-resolution scanning electron microscope images. J Microsc. 161, 343-355.

Lindroth M, Sundgren J-E. (1989). Ion beam-sputtered and magnetron-sputtered thin films on cytoskeletons: A high-resolution TEM study. Scanning 11, 243-253.

Luo S, Joy DC. (1988). Monte Carlo calculations of secondary electron emission. Scanning Microsc.2,1901-1915.

MacKenzie AP.(1972). Freezing, freeze drying, and freeze substitution. Scanning Electron Microsc.1972,273-280.

Moor H. (1973). Evaporation and electron guns. In: Benedetti EL, Favard P (eds) Freeze etching techniques and applications. Societe Francaise de Microscope Electronique, Paris. 27-30.

Mueller M, Marti Th, Kriz S. (1980). Improved structural preservation by freeze substitution. Proc 7th Europ Congr on Electron Microscopy, The Hague. The 7th Europ Congr on EM Foundation, Leiden. 2: 720-721.

Mueller M, Walther P, Hermann R, Schwarb P. (1989). SEM immunochemistry with small (5 to 15 nm) colloidal gold markers. In: Verkleij AJ, Leunissen JLM (eds). Immuno gold labelling in cell biology. CRC Press Inc, Boca Raton, Florida. 199-216.

Mueller M, Hermann H. (1990a). Towards high resolution SEM of biological objects. Proc XII Intern Congr EM, Seattle. San Francisco Press, Inc. 3: 4-5.

Mueller M, Hermann H. (1990b). Towards high resolution SEM of biological objects. Hitachi Instrument News, Electron Microscopy Edition. 19, 50-57.

Nagatani T, Saito S, Sato M, Yamada M. (1987). Development of an ultra high resloution scanning electron microscope by means of a field-emission source and in-lens systerm. Scanning Microsc. 1, 901-909.

Niedrig H. (1978). Physical background of electron backscattering. Scanning, 1, 17-34.

Osumi M, Baba M, Naito N, Taki A, Yamada N, Nagatani T. (1988). High resolution, low voltage scanning electron microscopy of uncoated yeast cells fixed by the freeze substitution method. J Electron Microsc. 37, 17-30.

Osumi M, Yamada N, Kobori H. (1990). Biological application of ultrahigh-resolution low-voltage scanning electron microscope, S-900LV. Hitachi Instrument News, Electron Microscopy Edition. 19, 38-44.

Pawley JB. (1972). Charging artifacts in the SEM. Scanning Electron Microsc. 1972, 153-160.

Pawley JB, Erlandsen SL. (1989).The case for low voltage high resolution scanning electron microscopy of biological samples. Scanning Microsc. Supplement 3, 163-178.

Pawley JB. (1990). Practical aspects of high-resolution LVSEM. Scanning. 12, 247-252.

Pawley JB, Walther P, Shih S-J, Malecki M. (1991). Early results using high resolution, low voltage, low temperature SEM. J Microsc. 161, 1-7.

Peters K-R. (1985). Working at higher magnifications in scanning electron microscopy with secondary and backscattered electrons on metal coated biological specimens and imaging macromolecular cell membrane structures. Scanning Electron Microsc. 1985; IV: 1519-1544.

Peters K-R. (1986). Metal deposition by high energy sputtering for high magnification electron microscopy. In: Advanced techniques in Biological Electron Microscopy. III, Koehler JK (ed), Springer Verlag Berlin. 101-166.

Peterson JB, Heuser JR, Nelson DL. (1987). Dissociation and reassociaton of trychocyst proteins: biochemical and ultrastructural studies. J Cell Science. 87, 3-25.

Ris H. (1985). The cytoplasmic filament system in critical-point dried whole mounts and plastic embedded sections. J Cell Biol. 100, 1474-1487.

Sato M, Nakaizumi Y, Yamada M, Nagatani T. (1990). Development of a low accelerating voltage SEM (S-900H). Hitachi Instrument News, EM Edition. 19, 45-49.

Slot JW, Geuze HJ. (1984). Gold markers for single and double immunolabelling of ultrathin cryosections. In: Polak JM, Varndell IM (eds) Immunolabelling for Electron Microscopy. Elseviers Science Publishers B. V. 129-143.

Small EB, Wetzel B, Maugel TK, Meola P. (1980). Preliminary study of ciliates stained with silver albuminose (protargol) examined in the backscattered electron mode with the SEM. Scanning Electron Microsc. 1980; III: 543-548.

Sperling L, Tardieu A, Gulik-Krywicki T. (1987). The crystal lattice of Paramecium trichocysts before and after exocytosis by X-ray diffraction and freeze-fracture electron microscopy. J Cell Biol. 105, 1649-1662.

Tanaka K, Mitsushima A. (1984). A preparation method for observing intracellular structures by scanning electron microscopy. J Microsc. 133, 213-222.

Tanaka K, Mitsushima A, Kashima Y, Nakacera T, Ostake H. (1989). Application of an Ultrahigh-resolution scanning electron microscope (UHS-T1) to biological specimens. J Electron Microsc Tech. 12, 146-153.

Thornley RFM. (1960). Recent developments in SEM. Proc of the Europ Regional Conf on Electron Microscopy, Delft, 1960, I. De Nederlandse Vereiniging voor Electronenmicroscopie, Delft. 173-176.

Trejdosiewicz LK, Smoira MA, Hodges GM, Goodman SL, Livingstone DC. (1981). Cell surface distribution of fibronectin in cultures of fibroblasts and bladder derived epithelium: SEM-Immunogold localization compared to immunoperoxidase and immunofluorescence. J Microsc. 123, 227-236.

Vandenburgh DJ, Ackerley CA, Lynn DH, Anderson RC. (1987). The use of silver nitrate staining and backscattered electron imaging to visualize nematode sensory structures. Scanning Microsc. 1, 1881-1886.

Walther P, Ariano BH, Kriz S, Mueller M. (1983). High resolution SEM detection of protein A gold (15 nm) marked surface antigens using backscattered electrons. Beitr Elektronenmikrosk Direktabb Oberf 16: 539-545.

Walther P, Kriz S, Mueller M, Ariano BH, Brodbeck U, Ott P, Schweingruber ME. (1984). Detection of protein A gold 15 nm marked surface antigens by backscattered electrons. Scanning Electron Microsc. 1984; III: 1257-1266.

Walther P, Mueller M. (1985). Detection of small (5-15 nm) gold labelled surface antigens using backscattered electrons. In: Mueller M, Becker RP, Boyde A, Wolosewick JJ. (eds) Science of Biological Specimen Preparation. SEM Inc., AMF O'Hare (Chicago), Il 60666-0507,USA.1986, 195-201.

Walther P, Hentschel J.(1989). Improved representation of cell surface structures by freeze substitution and backscattered electron imaging. Scanning Microsc. Supplement 3, 201-211.

Walther P, Herter P, Hentschel H, Hentschel J. (1990). High-resolution SEM of kidney tissue using cryo-techniques. Proc XII Intern Congr EM, Seattle. San Francisco Press, Inc. 3: 8-9.

Wepf R, Gross H. (1990). Pt/Ir/C, A new powerful coating material for High resolution SEM. Proc XII Intern Congr EM, Seattle. San Francisco Press, Inc. 3: 6-7.

Wildhaber I. Gross H. Moor H. (1985). Comparative studies of very thin shadowing films produced by atom beam sputtering and electron gun evaporation. Ultramicrosc. 16, 321-330.

Discussion with Reviewers

K. Zierold: What is the optimal accelerating voltage (V_0) for imaging a biological bulk specimen coated by a thin platinum layer with high spatial resolution?
Authors: On an ideal test specimen (good electrical conductivity, not sensitive to the electron beam, low amount of backscattering from the inner part of the sample) the spatial resolution is mainly dependent from the diameter of the primary beam. This diameter is smaller at higher V_0 and enlarged at lower V_0. On an ideal test specimen such as metal coated proteins on a thin conductive film, therefore, a better spatial resolution is obtained at higher V_0 (e. g. 30 kV). However, most of the interesting biological bulk samples are very different from ideal test specimens: They tend to charge up; they are beam sensitive and backscattered electrons are also scattered from the bulk part of the specimen thereby causing beam damage and obscuring the high resolution surface image. All these negative effects are reduced by using low V_0, as summarized by Pawley et al. (1991). For BSE-imaging it is of special importance that at low V_0 a higher percentage of the leaving BSE are scattered at the platinum layer and not in the bulk of the sample. This effect increases the contrast of the BSE-signal, as shown in fig. 6. For practical work one has to find a compromise between these opposite effects. We choose 4 kV because the surface signal was much higher than at 20 kV. On the other hand we were still able to resolve the platinum grains and we do not expect to preserve biological structures smaller than the grain size. Therefore, a better spatial resolution than obtained at V_0 = 4 kV would provide no further biological information. However, this V_0 = 4 kV should not be taken as an absolute value. For another study using a different microscope and a different coating method another value of V_0 might be more suitable.

K.-R. Peters: How large is the probe diameter at 4 kV causing such serious degradation of the edge contours?
Authors: According to Nagatani (1987) the beam diameter for the Hitachi S-900 is about 0.4 nm at V_0=30 kV and about 1.2 nm at V_0=4 kV. In practical work, however, the beam diameter may be larger due to inadequate focussing and improper correction of astigmatism.

K. Zierold: Is platinum the optimal coating material for BSE imaging?
Authors: A coating material for BSE-imaging has to have a high atomic number (Z) in order to produce a high BSE-signal. The coat should also have fine grain size not to hide small biological structures. Both conditions are reasonably well approached by using ion beam sputtered platinum coats. However, finer grain sizes are obtained by electron gun evaporation of platinum/carbon or platinum/iridium/carbon (Wepf and Gross, 1990).

K.-R. Peters: What is the nature of the small 2 nm pattern revealed on the surface of platinum/carbon coated cells (Fig. 3) compared to that of the grain structure seen in other images (Fig. 4 -6)?
Authors: The pattern in fig. 3 is obtained by electron gun evaporation of platinum/carbon, the grain structure in the figs. 4 -6 is obtained by ion beam sputtering of platinum. Currently, at this level of resolution (2 nm), we do not know whether the grain structures contain information about the underlaying biological sample.

K. Zierold: Can imaging of uncoated biological bulk specimens be improved by use of low accelerating voltage (V_0), perhaps supported by an additional positive electrical voltage at the specimen?
Authors: Imaging of uncoated bulk biological samples is certainly improved by use of low V_0 at least at low and intermediate magnifications. However, we never obtained convincing results at higher magnifications using SE, most probably due to local charge-up. To our understanding an additional positive voltage at the specimen hinders the SE1 and SE2 electrons to leave the sample. The image is formed by SE3 electrons that are produced by BSE and therefore less affected by specimen charge-up. (An example for this effect is presented in Walther and Mueller, 1985.) Since a sensitive BSE-detector is now available, it is probably more straight forward to directly use BSE. Fig. 16 shows a portion of a sea urchin embryo cell that was high pressure frozen, freeze fractured and imaged in the SEM after partial freeze-drying at 160 K using a cold-stage. No coating and no chemical treatment was applied. The figure is a BSE-image at V_0 = 3 kV. A nucleus, the two nuclear membranes and different other organelles can be seen. On such an uncoated bulk sample the resolution is mainly limited by the extraction depth of the BSE which depends from V_0. Therefore we expect to obtain better resolution by using even lower V_0. Unfortunately, sensitivity of the used BSE-detector drops below 3 kV. It would be a challenging task to develop a BSE-detector for an in-lens type SEM that is fully sensitive at 1 kV.

Fig. 20. Low voltage (V_0=3kV) BSE-image of an uncoated sea urchin embryo cell. The sample was high pressure frozen, freeze fractured and imaged after partial freeze drying at 160 K using a cold stage. No coating and no chemical fixation was applied. The two membranes of the nuclear envelope and different organelles are visible. No serious charging artifacts are present.